CHAPTER 1

INTRODUCTION

In recent decades, nanocrystalline semiconductors with different sizes and shapes have attractively studied because of the potential to design new materials and devices in various fields such as catalysis, medicine, cosmetic, electronic and etc [1, 2, 3]. Among them, nanostructured semiconductor transition metal chacoginides, such as CdS, CuS, ZnS, PbS, Bi_2S_3 and Sb_2S_3 have been extensive studied for nanoscience including nanotechnology because of their special physical and chemical properties, and their technological applications. Recently, metal sulfide nanostructures have attractive considerable research activities due to their great potential for fundamental studies of the roles of dimensionality and size in their physical properties as well as for applications in optoelectronic nanodevices and functional materials [4, 5].

It is well known that the controllable size and shape are the prerequisite for the study and application of metal sulfides. As a result, many methods have been developed to prepare metal sulfide nanostructures ranging from milling techniques to chemical and lithographic methods. Their main weaknesses are, however, attributed to poor control of morphology of the final products [6]. Various approaches, such as liquid crystal templates [7], irradiations [8], electrochemical reactions [9], polymer controlled growth [10], electrodeposition on a porous templates [11], and solvothermal routes [12] have been applied to achieve various metal sulfide nanostructures. Among these synthesis approaches, solvothermal have been applied to improve quality of metal sulfides such as crystallinity, monodispersity and others. In

addition, this method is ideal for industrial synthesis with their low cost and maneuverability. For instance, Qian's group obtained CdS nanorods by solvothermal method using ethylenediamine as the coordinating solvent and the template [13-15].

The solvothermal processing of materials is a solution processing and can be described as super heated aqueous solution processing. This process takes place in a liquid medium above the boiling point and atmospheric pressure. Crystallization by solvothermal synthesis is, in the simplest case, a straight forward of isothermal equilibrium reaction. Substances that are insoluble under ambient conditions are dissolved, and the crystalline phase, which is stable under the solvothermal conditions, forms. Most of the solvothermal processes are carried out in water, and thus are termed hydrothermal. Besides water, alcohol, ammomia, ethylenediamine and others are the most important solvothermal reaction media [16-17].

For the present research, the architectural control of metal sulfides nanostructure with well defined shapes is an important goal of my research because of the importance of the shape and textures of materials in determining their widely varying properties [18]. Although there has been an increasing number of excellent studies on novel nano- and microstructured materials with various shapes, such as low-dimensional structures (e.g., rods, wires, belts, tubes, cubes) and hierarchical structures (e.g., dendrites, branches, urchins, networks), the ability to understand and predict the final structures is still limited. Herein, various kinds of metal sulfides such as CdS, CuS, Bi_2S_3 were synthesized using a growth controlling agents via a solvothermal method as well as study growth process. If we could understand the growth mechanism and the shape-guiding process, it will be possible for us to program the system to yield the crystals with desired shape and crystallinity.

1.1 Crystal structures of metal sulfides

1.1.1 Cadmium sulfide (CdS)

Cadmium sulfide (CdS) is a semiconductor which has a direct band gap semiconductor (2.42 eV) and has many applications for example in light detectors photovoltaic and etc. CdS has two crystal forms; the more stable hexagonal wurtzite structure and the cubic zinc blend. In both of these forms the cadmium and sulfur atoms are four coordinates [19].

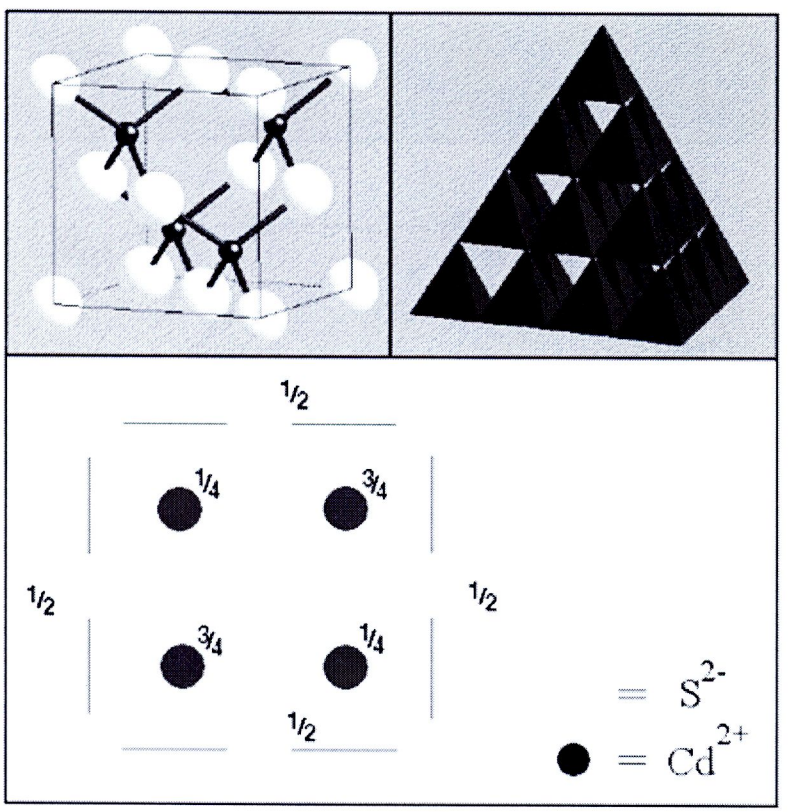

Figure 1.1 Sphalerite structure of CdS and its projection representation [19]

The sphalerite structure (Figure 1.1), which is known as the zinc-blend structure, is based on a cubic closed pack (ccp) array of bulky anions (S^{2-}) but cations (Cd^{2+}) occupy one type of tetrahedral hole, one haft the tetrahedral holes present in a close-

packed structure. Each ion is surrounded by neighbours and so, the structure has (4, 4) - coordination. In this notation, the first number in parenthesis is the coordination number of the cation, and the second number is the coordination number of the anion.

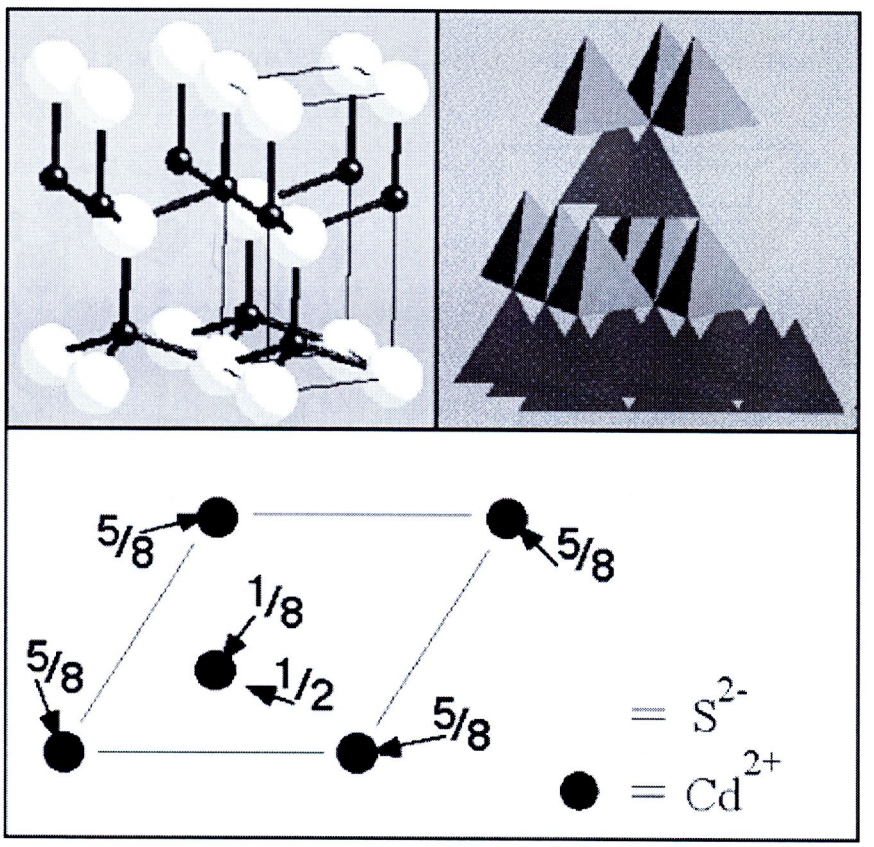

Figure 1.2 Wurtzite structure of CdS and its projection representation [19]

The wurtzite structure (Figure 1.2) differs from sphalerite structure in being derived from an expanded hexagonal closed pack (hcp) anion array rather than a ccp array, but as in sphalerite the cations occupy one type of tetrahedral hole. This structure has (4, 4) - coordination as same as sphalerite structure. The local symmetries of cations and anions are identical towards their nearest neighbours in wurtzite and sphalerite but differ at second - nearest neighbours [20].

1.1.2 Copper sulfide (CuS)

Copper sulfide or CuS (refered to as covellite or covelline) crystallizes in hexagonal crystal system corresponded to $P6_3/mmc$ space group with 6 formula units (12 atoms) per unit cell in which Cu atoms have tetrahedral and trigonal planar coordination and S atoms have tetrahedral and trigonal bipyramidal coordination.

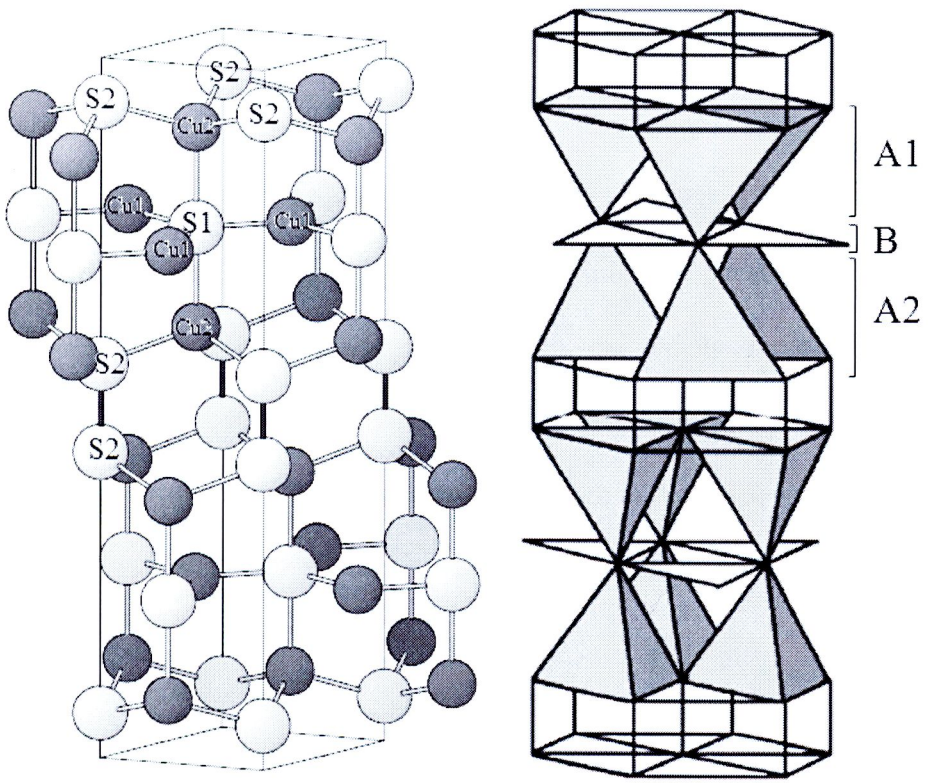

Figure 1.3 Crystal structures of CuS and the arrangement of Cu (dark) and sulfur (light) atoms [21]

The crystal structure of CuS can be presented as "sandwich" or packet, which consists of three alternating layers A_1-B-A_2 (Figure 1.3). The layers A_1 and A_2 are made up of CuS_4-tetrahedra, jointed by vertexes. The layer B represents the net of CuS_3- triangles, combined by apexes. In frame of packet the CuS_4-tetrahedra of layers A_1 and A_2 are turned in opposite directions. Usually, three sulfur atoms of CuS_3-

triangle are referred to as S(1), one of them is common with CuS_4-tetrahedra. Other sulfur atoms of CuS_4-tetrahedra are referred to as S(2). Copper atoms in triangular and tetrahedral coordination are marked as Cu(1) and Cu(2), respectively. The packets A_1-B-A_2 are connected together along the *c*-axis by S(2)-S(2) bonds ("dumbbells") [21].

1.1.3 Bismuth sulfide (Bi_2S_3)

Bismuth sulfide (Bi_2S_3) crystallizes in the orthorhombic crystal system with Pbmn. This compound has sheet type structures with the infinite chains along c axis (as shown in Figure 1.4). There are two sheets per unit cell. The Bi–S interactions along the infinite chains are mainly covalent, while the sheets (layers) are held together with weaker interatomic forces (Van der waals force). The shortest interatomic distances between the ribbons in *b* direction are about 1.5 times larger than those in the structure. This leads to easy cleavage in the (010) -plane [22-23].

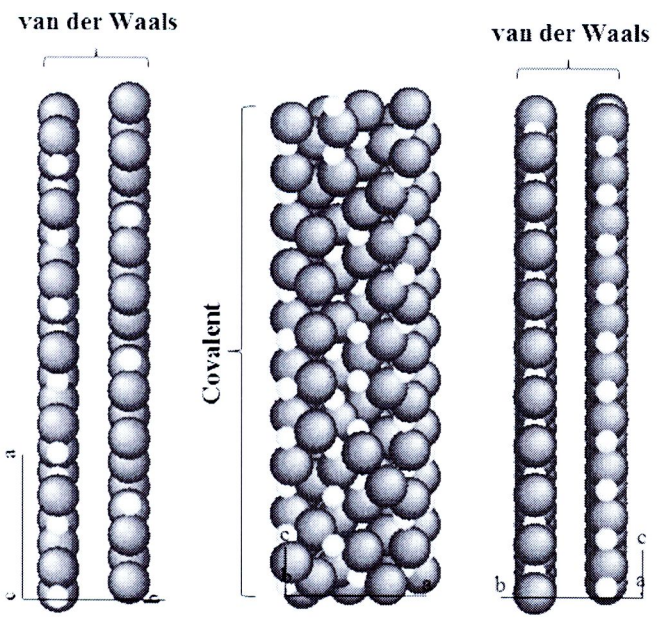

Figure 1.4 Computer modeling of Bi_2S_3 structure projected along 001, 010 and 100 directions. (The black balls represent S^{2-} ions and the white balls represent Bi^{3+} ions) [24]

1.2 Unique properties of anisotropic nanostructures and their application

Anisotropic nanocrystals are building block for new electronic and optical devices such as quantum computers, light emitting diodes, solar cells or lasers. Such devices frequently require sophisticated nanocrystals with morphogies that are not spherical. One such example is bulk heterojunction solar cells, where nanowires are predicted to result in an improved performance. In particular, one - dimensional (1D) and two-dimensional (2D) nanostructures are attractive candidates for nanoscience studies as well as nanotechnology applications such as nanoelectronics, nano-optoelectronics, nano- electromechanical systems [25].

1.2.1 One-dimensional (1D) nanostructures

1D nanostructures are those in which crystallite size are negligible in two dimensions but is not confined in the third ones; that is, electron and hole motion are confined in two spatial directions while free propagation is allowed in the third direction. This allows them to be used in applications where electrical conduction rather than tunneling transport is required. Because of the unique density of their electronic states in the limit of small diameters, they are expected to exhibit significantly different optical, electrical and magnetic properties from their bulk counterparts [26]. In addition to very high density of electronic states and joint density of states near the energies of their Van Hove singularities of these nanostructures, they have some of the way which these differ from bulk materials such as increased surface area, enhanced exciton binding energy, diameter-dependent bandgap and increased surface scattering for electrons and phonons. The examples of 1D nanostructure are nonowires, nanorods and etc.

In other words, 1D nanostructure is an electrically conducting wire or rod in which quantum effects control the transport properties in two dimensions. Owing to the confinement of conduction electrons in the transverse direction of this material, their transverse energy is quantized into a series of discrete value E_0, E_1,....E_n(" ground stage" energy with lower value). One consequence of this quantization is that the resistance of this structure cannot be deducted from classical formula:

$$\Omega = \rho\,(L / A)$$

where ρ is the resistivity, and L and A are length and cross-sectional area of nanorods or nanowires, respectively. For such structures, an exact calculation of the transverse energies of the confined electrons has to be accomplished to find the resistivity of this structure. Following from the quantization of electron energy, the resistance is, naturally, also quantized. The strength of the influence of quantization is inversely proportional to the diameter of this structure.

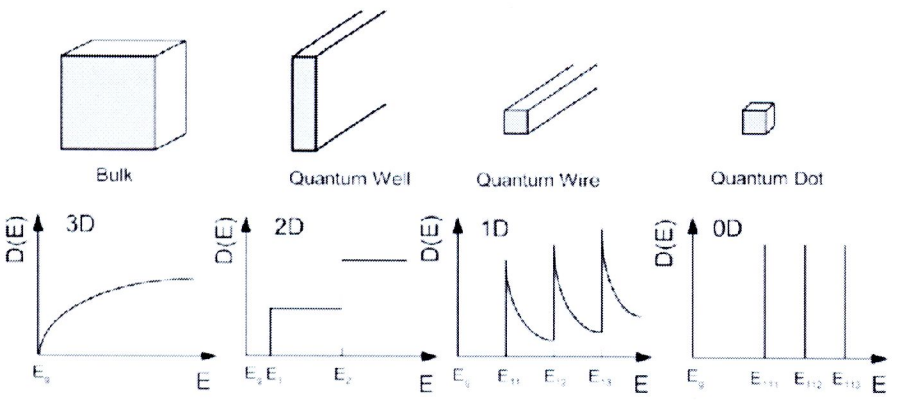

Figure 1.5 A schematic illustration of density of states (DOS) distribution in a bulk (3D), quantum well (2D), quantum wire (1D) and quantum dot (0D) [26]

Physical Properties and Phenomena [27]

Optical Preperties. 1D nanostructures are promising for optical application. These systems exhibit a singularity in their joint density of states, allowing quantum effects in them to be optically observable at room temperature. Since their density of states (DOS) in the quantum limit is highly localized in energy, the available state quickly fill up with electron as the intensity of the incident light is increased. This filling up of the subbands, as well as other effects those are unique to low-dimensional materials, lead to strong optical non-linearity in quantum nanostructures.

Light emission from one-dimension nanostructures can be achieved by photoluminescence (PL) or electroluminescence (EL), distinguished by whether the electronic excitation is achieved by optical illumination or by electrical simulation across a p-n junction, respectively.

Optical application of one-dimensional nanotructures has been extensively studied by a number of research groups for example, light emitting diode (LED), semiconductor nanowire lasers, ultrashort optical pulse generation, photodetectors. Furthermore, these structures have been shown to provide a promising framework for applying the "bottom-up" approach to the design of nanostructures for nanoscience investigations and for potential nanotechnology applications.

Mechanical Properties. There is much interest in the use of nanowires or nanorods as connectors in electrical devices. Nanomechanical measurements using AFM tip found that in Au nanowires, Young's modulus is independent of diameter and that yield strength is the largest for the smallest tubes with strengths up to 100 times better than that demonstrated by bulk materials.

Ballistic Conduction. Ballistic conduction occurs when the length of the conductor is smaller than the mean free path of the electron. In the other words, electrons are allowed to flow without collisions with phonons, impurities, etc. No energy is dissipated during the electrical conduction process. The lack of impurities that cause elastic scattering in the conduit material is imperative for this to occur; loss of quantization results if this happens.

1.2.2 Two-dimensional (2D) nanostructures [27]

2D nanostructures are those in which the crystallite size is negligible in one dimension and is not restricted in the other two directions; electron and hole motion is confined in only one spatial direction, whereas free propagation is allowed in the two spatial directions. There are also called *quantum wells.* Therefore, a quantum well can be defined as a structure where one dimensions is comparable to the exciton Bohr radius.

Since particle motion is confined to two dimensions, the geometric correlation is to that of a plane with no thickness. When the quantum well thickness is comparable to the Broglie wavelength of the carriers (i.e., electron and holes), just like with zero- and one-dimensional materials, quantum confinement take place in that material in just one dimension that normal to the surface of the material.

A simple approximation of the energy of the square quantum well with thickness L that is comparable to the de Broglie wave length of the carriers (generally electrons and holes) is

$$E_n = (\hbar^2\pi^2/2mL^2)\, n^2$$

Physical Properties

Optical Properties. Optical properties depend on several parameters: (1) composition, (2) thickness, and (3) structure (orientation). These, in turn, affect properties such as interference, reflectivity, absorption, and the refractive index. All of these characteristics also depend on the kind of decomposition mechanism. If the substructures are small enough, it is not scatter light. This structure can be hydrophilic or hydrophobic.

Mechanical Properties. Mechanical properties of this structure is differ bulk material counterparts because of their unique nanostructure and because they possess inherently large surface-to-volume-ratio.

1.2.3 Applications

Light Emitting Diodes (LEDs)

Semiconductor NCs have been explored as the emitters for thin film light-emitting diodes (LEDs) [28-29]. In a typical LED, a thin layer of light-emitting NCs, for example, CdSe/ZnS core-shells or $Cd_{1-x}Zn_xSe$ (recombination layer), is sandwiched between the hole transport layer (HTL) and electron transport layer (ETL), which provide injection of carriers into the NCs (Figure 1.6). The performance of NCs-based LEDs has remarkably improved over the past decade. Among them, strong points of NC-based LEDs are their high color purity (i.e., narrow emission band) and tunability of the emission color from UV to near-IR by simply varying the NC size and shape. [30-31]

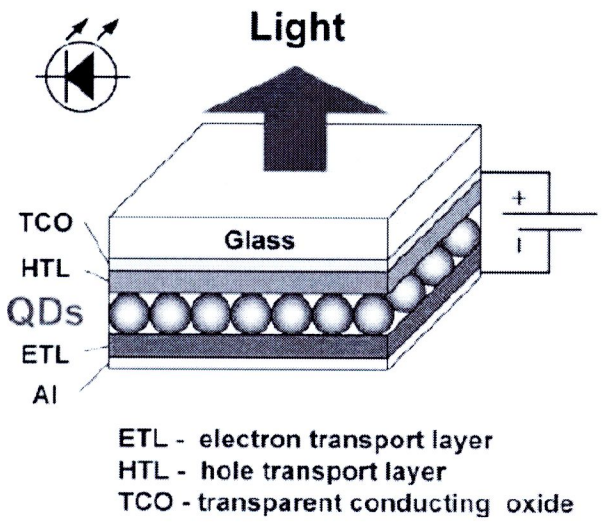

Figure 1.6 Schematic diagram and a typical structure of a thin film LED utilizing semiconductor NCs [30]

Semiconductor NCs have been used for LED application in two ways. First, they are used to enhance light emission of LED devices with other materials, for example, conjugated polymers, as the active media. The role of the semiconductor NCs is not completely clear but thought to enhance either charge injection or transport. In some cases, the presence of semiconductor NCs in carrier-transporting polymers has been found to not only enhance the photoinduced charge generation efficiency but also extend the sensitivity range of the polymers, while the polymer matrix is responsible for charge transport. This type of polymer/nanocrystal composite materials can have improved properties over the individual constituent components and may have interesting applications. Second, the semiconductor NCs are used as the active materials for light generation directly. In this case, the electron and hole are injected directly into the CB and VB, respectively, of the NCs and the recombination of the electron and hole results in light emission. Several studies have been reported with the goal to optimize injection and charge transport in such device structures using CdS

and CdSe nanoparticles. Since the mobility of the charge carriers is usually much lower than in bulk single crystals, charge transport is one of the major limitations in efficient light generation in such devices. For example, photoconductivity and electric field induced PL quenching studies of close-packed CdSe quantum dot solids suggest that photoexcited, quantum confined excitons are ionized by the applied electric field with a rate dependent on both the size and surface passivation of the quantum dots. Separation of electron–hole pairs confined to the core of the dot requires significantly more energy than separation of carriers trapped at the surface and occurs through tunneling processes. New nanostructures such nanowires, nanorods, and nanobelts may provide some interesting alternatives with better transport properties than nanoparticles. Devices such as LEDs and solar cells based on such nanostructures are expected to be developed in the next few years [32].

Photodetectors

There is a large variety of sensitive photon detection systems operating in the visible spectral range: photomultiplier tubes, single crystal silicon detectors, and CCD cameras. Unfortunately, in the infrared the situation is not nearly as good; available detection systems, especially array based, are either insensitive or very expensive. The reason is simple; silicon, which is a main workhorse for CCD and APD technologies cannot operate beyond 1.1 μm, whereas other materials show higher noise levels or are difficult to process using standard single-crystal-based microfabrication techniques. At the same time, markets for near-IR and mid- IR detectors span from telecommunication to night-vision systems, bioimaging, environmental sensing, spectroscopy, and chemical analysis. For all of those areas, it is highly desirable to

find new materials that enable high detectivity at a reasonable cost. Recent developments provide good expectations for photodetectors based on NC solids.

Application of NCs for photon detection is receiving steadily growing attention. The progress in this direction is driven by the unique opportunities given by the size-tunable NC electronic structure, NC surface chemistry, and surface trap engineering, compositional flexibility, and the possibility to manufacture devices using inexpensive solution processing. Relatively wide band gaps of conductive organic polymers and small molecules limit their absorption to visible spectral range. For applications requiring light absorption/emission in the near-IR region, inorganic NCs, especially those made of narrow-gap PbS, PbSe, PbTe, Bi_2S_3 and Sb_2S_3 semiconductors, are in strong position to compete with other technologies, because their band gap can be precisely tuned from the visible spectral region upto the wavelengths of 3500 nm [33].

Recently, Researchers present several examples of photodetectors using blends of NCs with organic materials. In these systems, the use of NCs allowed one to obtain higher responsivity or extend spectral response to the infrared spectral region. Small molecules such as fullerene derivatives or π-conjugated polymers are known as light-sensitive materials suitable for fabrication of solar cells and photodetectors. However, their spectral response is limited to the visible spectral region. Narrow gap NCs can be an excellent sensitizer when blended with semiconducting organic materials. The concept of hybrid organic-NC devices was used to examine synergistic light harvesting and charge transport. For example, 3 orders of magnitude enhancement of photocurrent was achieved by sensitizing crystalline arrays of C_{60} with CdSe NCs [34]. This enhancement was explained by efficient light absorption of CdSe NCs, fast

electron transfer from NCs to C_{60}, and high carrier mobilities within the array of C_{60} molecules. A similar idea, but for the IR range, was demonstrated by combining PbS NCs and soluble C_{60} derivative, [6,6]-phenyl-C61-butyric acid methyl ester (PCBM). Interestingly, the films of untreated, oleic acid capped PbS NCs are highly insulating and show very poor photoresponse. However, composite solids made of PbS/PCBM in a 1:1 weight ratio exhibited $D^* \approx 2.5 \times 10^{10}$ Jones and $i_{ph}/i_d \approx 104$. Importantly, spectral response follows the absorption spectrum of PbS NCs with cutoff wavelength in the near-IR. Reference samples of pure PCBM exhibited 2-3 orders of magnitude lower responsivity. These results combined with time-resolved luminescence and transient absorption measurements were explained by the efficient electron transfer from PbS NCs to PCBM [35].

Photovoltaic Cells (PV)

Photovoltaic cell is a device that can convert sunlight directly into electricity and are often used in various areas for example in space, in home, on the sunroof of car, on the road and etc. Photovoltaic cell is one of the most promising renewable energy technologies for this century because it is abundant resource and has possibility for solving environmental problem. The growing demand for renewable energy requires significant efforts to be invested in the development of efficient and inexpensive photovoltaic materials. Semiconductor NCs are considered promising candidates for photovoltaic applications due to the combination of superior optical and electronic properties of inorganic semiconductors with the opportunities for inexpensive, solution-based device fabrication. NC-based photovoltaics are probably the most desired kind of NC devices that can make a really significant technological impact.

Many efforts have been expended on the semiconductor-sensitized analogue (SSSC), where a light-absorbing semiconductor deposited on the porous transparent oxide takes the place of the dye in Dye-sensitized solar cell (DSSC). The use of a semiconductor instead of a dye is often perceived to impart some advantages to the cells, mainly higher absorption (typically by a factor of 5-7) of the semiconductor coating compared with a single molecular layer of dye; greater stability of the semiconductor compared to organometallic or even pure organic dyes; and tailoring of optical absorption over a wider wavelength range than possible with dyes due both to the inherently wider bandgap range of semiconductors as well as the ability to tailor the bandgap by size quantization. More recently, the possibility of exploiting multiple exciton generation to obtain high efficiencies adds another potential advantage that could be exploited in the future. However, in spite of these potential advantages, the solar efficiency of liquid junction SSSCs has reached only 4.15% at present [36]. Although the DSSC does possess some fundamental advantages, we can expect large improvements in efficiency of the SSSC, possibly reaching values comparable to the DSSC [37].

There are different approaches used to employ semiconductor nanocrystals in photovoltaic cell for example;

Nanocrystals in Hybrid Bulk Heterojunction Solar Cells

Semiconductor nanocrystals are regarded as useful materials for building hybrid organic–inorganic so-called bulk heterojunction donor-acceptor solar cells. This utility is due to the fact that their optical band can be tuned by both material selection and quantum confinement and because advances in synthesis allow control over nanocrystal size and shape to optimize performance. Other advantages of using

nanostructured layers in thin film solar cells are (a) the optical path for photon absorption is increased than the actual thin film thickness due to multiple reflections and (b) light generated from electrons and holes need to travel over a short path therefore, recombination losses are greatly reduced and consequently, the absorber layer thickness in nanostructured solar cells can be as thin as 150 nm instead of several microns in traditional solar cells. To obtain high efficiencies, it is necessary to have an interpenetrating network of electron-accepting and hole-accepting components within the device which are achieved using polymer blends or a mixture of conjugated polymers with C_{60} derivatives. As a result, the use of nanocrystals is particularly attractive in hybrid nanocrystal-polymer cells because different sizes and different shapes can be used to improve charge transport and energy conversion [38]. The cells with single active layer can achieve power conversion efficiency of about 5% [39]. Efficiency of ~7% was demonstrated for a tandem solar cell with different band gaps [40]. The outdoor lifetime of such solar cell was found to be more than 1 year. However, the main factors limiting the performance of polymer solar cells are chemical and photochemical stability of polymers and contacts as well as relatively poor electronic properties of organic materials.

The performance of such solar cells can be improved by extending nanocrystal absorption into the IR region by using narrow band gap semiconductors [41]. Narrow gap semiconductor NCs has been used in hybrid photovoltaic cells to harvest infrared part of solar spectrum [42-43].

Colloidal Nanocrystals for All-Inorganic Solar Cells

As describe above, the use of inorganic nanocrystals (NCs) for electron transport can enhance the performance of semiconductor polymer solar cells [44] but the ultimate limitations of these hybrid systems may still be dictated by the low mobility and environmental sensitivity of their organic phase. Recently, All-inorganic solar cells made of colloidal NCs could avoid unstable organic components while keeping the benefits of solution-based device fabrication, for example, A. Paul Alivisatos et al. introduces solar cells based entirely on colloidal semiconductor nanocrystals. They are ultrathin, solution processed, and stable in ambient environments. Sintering is found to enhance the performance of these devices, allowing for air-stable power conversion efficiencies up to 2.9%. This nanocrystal solar cell offers an exciting research direction and serves as a key development toward achieving stable and low cost solar energy conversion [45].

In addition to electronic or optical applications, semiconductor nanostructures have also been used to medical applications for example, biomolecule-associated nanocircuits, sensor, drug delivery and etc [46-47]. Semiconductor nanostructures are the most extensively studied compound because of the versatile size-tunable properties of its nanostructures. Especially, one dimensional nanostructure, this structure is able to prevent reduction in signal intensities which are innate to higher-dimensional structures. This property of the one-dimension nanostructures provides a sensing modality for label-free and direct electrical readout when the nanostructure is used as a semiconducting channel of a chemiresistor or field-effect transistor. This type of label-free direct detection is especially advantageous for rapid and real-time monitoring of receptor-ligand interactions with receptor-modified nanostructure. This

is particularly true when the receptor is a biomolecule such as antibody, DNA, or protein. In the future, this procedure could prove to be critical for accurate clinical diagnosis [48].

1.3 Shape-controlled synthesis

In this section, the synthetic methods developed in recent year to control the shape of metal chacogenides will be mentioned.

1.3.1 High-temperature organometallic routes

In the pioneering work, researcher reported a method for the synthesis of high quality nanoparticles of cadmium chalcogenides based on the high-temperature nucleation and growth of nanoparticles from organometallic precursors. The resultant nanoparticles were of high quality and had a spherical morphology. There was further pioneering work from the group of Alivisatos that induced anisotropy in cadmium chalcogenides nanoparticles. They prepared the nanorods by using a mixed-surfactant system, that is, tri-octylphosphine oxide (TOPO) and phosphonic acids. The nanorods displayed many important property modifications compared to nanodots, such as polarized light emission. With the modification, the groups of Peng and Alivisatos were able to synthesize cadmium chalcogenides nanoparticles of various other morphologies, such as arrows, pine trees, teardrops, and tetrapods. In addition, there have been reports of several other studies to synthesize anisotropic II-VI semiconductor nanooparticles using mixed-surfactant systems for nanocrystal growth [49-50]. The formation of anisotropic nanoparticles in monosurfactant systems could be obtained in ethylenediamine [51]. Even though the exact mechanism of shape evolution was not fully explained, they observed that this ligand was unique; it was not possible to replace ethylenediamine with other ligands such as pyridine or

diethylamine. The results described above indicate that the nature of the surfactant plays an important role in determining the shape of nanoparticles. In some recent reports, anisotropic metal chacogenides nanocrystals in single-surfactant systems, namely, TOPO or hexadecylamine (HDA) was prepared. In these systems, it is possible that surfactant molecules build molecular templates within which the nanoparticles grow, a scenario similar to that where nanoparticles are formed in micellar systems. A possible model for such nanoparticle growth is shown in Figure 1.7 Due to the reduced steric hindrance between the hydrocarbon units of HDA, the packing density at the surface of the initially formed nanocrystal nuclei is greater than that of TOPO-coordinated nanocrystals. This leads to a reduced curvature on the growing crystallite surface, and finally to anisotropic growth in HDA-capped nanoparticles. Depending upon the type and nature of the surfactant, various morphologies of nanoparticles can be prepared.

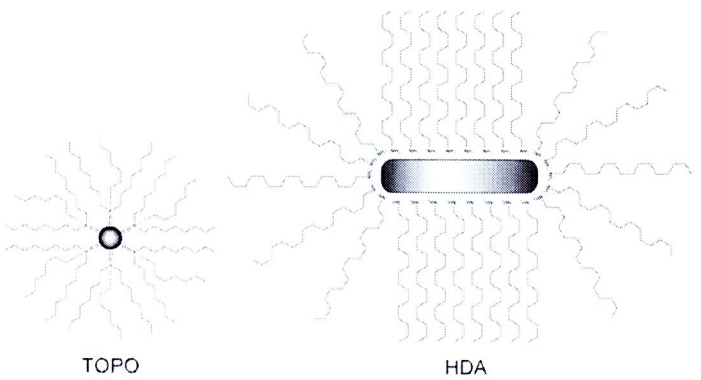

Figure 1.7 A possible template mechanism for the growth of nanoparticles in monosurfactant systems, namely, TOPO and HAD [25]

Some researcher has used this method to synthesize metal chaclgenides with complex morphologies for example tetrapods by taking advantage of the concept of

low stacking-fault energy differences between the wurtzite and sphalerite (Figure 1.8). In this class of nanocrystals, it was observed that the core of the tetrapod possessed a zinc blende structure while the arms exhibited the wurtzite modification. They proposed that to successfully grow the tetrapods, crystallites must nucleate in the sphalerite phase. The sphalerite structure has a tetrahedral geometry with four arms pointing along the vertices of a tetrahedron. It follows that these (111) zinc blende faces are common with the (002) face of the wurtzite lattice. By changing the temperature, growth of the the wurtzite phase along the crystallographically similar (002) direction can be induced, which is responsible for the growth of the arms of the tetrapods. Therefore, by changing the growth temperature one can play with the growth process, so as to produce either the wurtzite or sphalerite modification. If the arms are purely wurtzite they will grow straight. However, it has been observed that the stacking fault energy between the wurtzite and sphalerite modifications of the cadmium-based chalcogenidesis of the order of few eV. Thus, by changing the reaction parameters, stacking faults can be induced and one can manipulate nanoparticle growth between wurtzite and sphalerite modifications. The presence of stacking faults near the ends of the arms may lead to the further branching of the tetrapods and more complex shapes such as dendritic tetrapods can be synthesized. A model for such a growth mechanism is shown in Figure 1.8. This anisotropic growth is fast at high concentrations of precursors, which provides the monomers required for the growth of semiconductor crystallites [52].

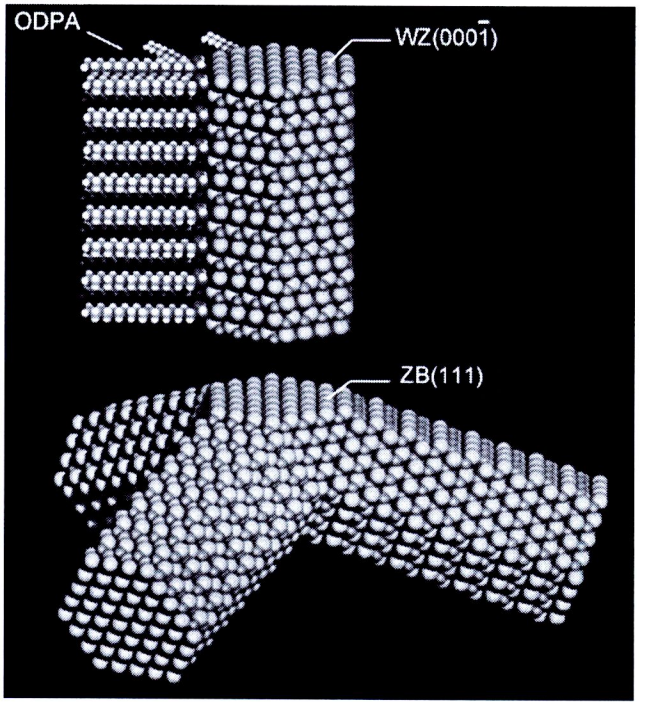

Figure 1.8 A possible model for CdE (E =S, Se, Te) tetrapod [52]

At low precursor concentrations, the diffusional flux of monomers to the growing crystallite surface is reduced and the reaction system tends towards a thermodynamically controlled regime, which results in spherically shaped nanocrystals. The role of the injection method was examined for chalcogenides. It was observed that the rate of injection of the chalcogenide precursor has a significant effect on the shape of the nanoparticles. At high injection rates, spherical nanoparticles were achieved. It can be shown that by simply injecting chalcogenide precursors in a stepwise manner, selective epitaxial deposition on the (002) surface can be promoted to elongate the initial nuclei into nanorods. At present, the exact reaction mechanism for the formation of anisotropic nanoparticles is still un- known. In order to describe the synthesis of these nanocrystals, one should carefully evaluate the role of surfactants, temperature, monomer concentrations and growth time.

1.3.2 Single-source precursors

The single-source-precursor method is a deviation from the high-temperature method for the synthesis of semiconductor nanoparticles. In this method, the first step involves the synthesis of a single-source precursor in which both the metal and nonmetal component of the compound semiconductors are incorporated within a single molecule. The single-source precursor is then injected into a hot boiling solvent, where the thermal decomposition of the precursor generates the desired nanoparticles. The most commonly used precursor is $Li_2[Cd_{10}Se_4(SPh_{16})]$ that has been used to generate a number of Cd-based chalcogenides [53-54]. Some researchers used cadmium dithio- and diselenocarbamate complexes as precursors for the preparation of TOPO-capped II-VI semiconductor nanoparticles [64-65]. This method eliminates the need for volatile metal alkyls, however they were air sensitive. Attempts were carried out to synthesize air stable single-source precursors for example diselenocarbamate complexes, xanthates complexs and etc [55-56]. One of the main disadvantages of the single-source-precursor method is that the nanoparticles, in general, do not exhibit particularly good luminescence properties, and are often polydisperse in nature.

1.3.3 Micellar methods

The micellar method is a very important route for preparing semiconductor nanocrystals [57]. The inverse-micelle method has the advantage that the surface of the crystallites can be passivated or capped in a secondary reaction. The addition of selected surfactants to alkanes containing traces of moisture results in the spontaneous formation of inverse micelles. These inverse micelles are small surfactant aggregates with an aqueous core dispersed within the alkane media. The average size of the

micelles is controlled by the ratio of surfactant to water. Micelles serve as small reactor vessels that are loaded with metal salts: the addition of organically soluble chalcogenide reagents results in the formation of semiconductor nanoparticles [58]. Rapid loading of the organic phase is achieved by direct injection of the chalcogenide into the reaction vessel. Temporally discrete nucleation of nanoparticles occurs in the micelles with further growth limited by the diffusion of reagents through the micelle interface. The size of the micelle does not physically affect the size of the particles, rather it affects the spatial distribution of the reagents (the local concentration). The surfactant molecule temporarily coordinates to the surface of the formed particles and stabilizes the dispersion sterically.

Shape anisotropy in semiconductor nanoparticles was achieved using a combination of two surfactants: the anionic bis(2-ethylhexyl)sulfosuccinate (AOT) and the zwitterionic phospholipid L-α-phosphatidylcholine (lecithin) [59]. The change in particle morphology from spherical quantum dots to high-aspect-ratio quantum rods in this case is believed to be due to surfactant templating. Figure 1.9 illustrates a possible template mechanism. In the mixed-surfactant system, there would be a non-uniform distribution of surfactants, where AOT primarily occupies the regions of high curvature (around water) and lecithin occupies regions of low curvature. AOT would tend to cap the ends of wormlike micelles formed by lecithin, thus leading to the highly ellipsoidal droplet structure that templates the synthesis. Using a similar approach, triangular CdS nanocrystals were synthesized where equilateral CdS nanocrystals with 10 nm sides were produced in a $Cd(AOT)_2$/isooctane/water reverse micellar solution via a colloidal self-assembly approach [60]. The nanoparticles prepared via reverse micellar methods are in general of very weak luminescence and

of poor crystallinity. In addition, the size of the nanoparticles produced is rather restricted.

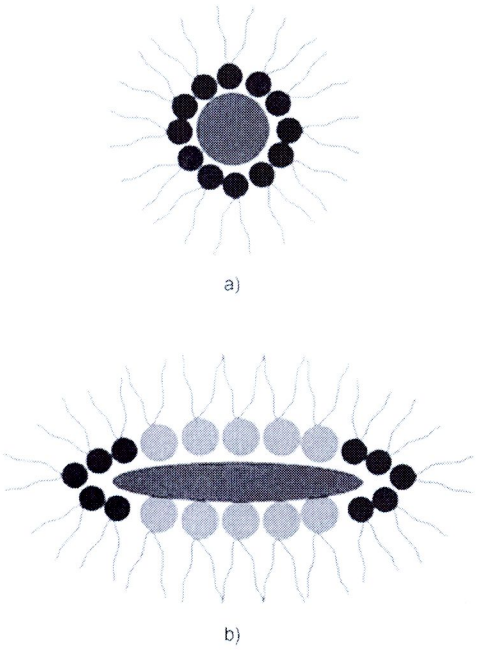

Figure 1.9 Template-directed mechanisms for nanoparticle growth in reverse micellar synthesis: a) nanoparticles; b) nanorods [59]

1.3.4. Catalytic-growth approach

Catalytic-growth approaches for the synthesis of metal sulfides via single-source-precursor methods were pioneered by the group of Lieber [61]. This approach is based on nanocluster-catalyzed vapor-liquid-solid (VLS) growth process. The key feature of this synthesis is the promotion of anisotropic crystal growth using metal nanoparticles as a catalyst. Three well-defined stages have been identified during the process: metal alloying, crystal nucleation, and axial growth, as shown in Figure 1.10.

In this mechanism, the role of the impurity is to form a liquid alloy droplet with a relatively low freezing point. The liquid droplet is an energetically favored site for

deposition from the vapor; the cluster supersaturates at these sites and grows a 1D structure of the material. The lower limit of the diameter is usually > 0.1 pm and is limited by the minimum diameter of the liquid metal catalyst that can be achieved under equilibrium conditions. They exploited the use of laser-assisted methods to prepare nanometer-scale catalyst clusters that subsequently define the size of the wires produced by the VLS mechanism. The generation of nanometer-sized clusters overcomes the limitation of equilibrium cluster sizes in determining the minimum wire diameters using the conventional VLS method. In this method, a pulsed laser is used to vaporize a solid target containing the desired material and a catalyst, and the resulting liquid nanoclusters formed at elevated temperature direct the growth and define the diameter of the crystalline nanowires through a VLS mechanism. A key feature of both the VLS growth process and the laser-assisted catalytic growth (LCG) processes is that equilibrium phase diagrams can be used to predict catalysts and growth conditions, and thereby enable a rational synthesis of new nanowire materials. In addition, some researchers have synthesized nanowires of CdS and ZnS using the single-source precursors $[Cd(S_2CNEt_2)_2]$ and $[Zn(S_2CNEt_2)_2]$, respectively. In this synthetic method, the single-source precursors undergo thermal decomposition in the growth region of a furnace, form M-S-Au (M = Cd or Zn) liquid solutions with the Au nanocluster catalysts, and then undergo nucleation and nanowire growth when the nanodroplets become saturated with reactants [62-63].

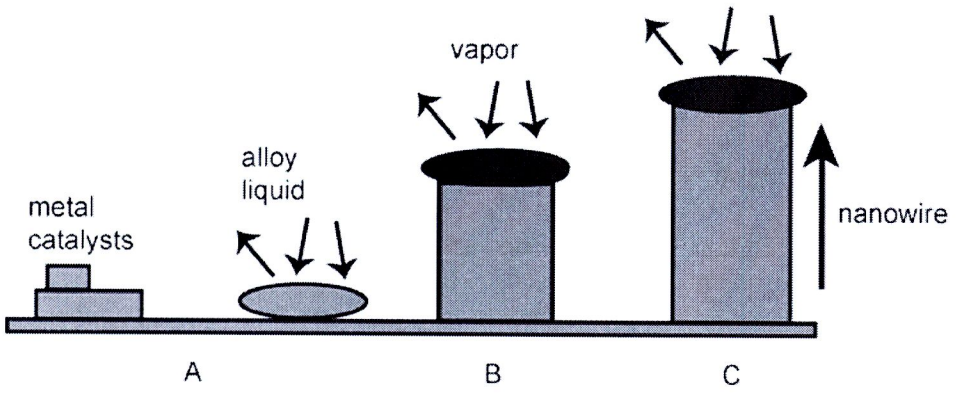

Figure 1.10 Schematic illustration of the vapor–liquid–solid nanowire growth mechanism comprising three stages: A) alloying, B) nucleation, C) axial growth [63]

1.3.5 Solvothermal synthesis

The solvothermal technique is becoming one of the most important tools for advanced materials processing, particularly owing to its advantages in the processing of nanostructural materials for a wide variety of technological applications such as electronics, optoelectronics, catalysis, ceramics, magnetic data storage, biomedical, biophotonics, etc. The sovolthermal technique not only helps in processing monodispersed and highly homogeneous nanoparticles, but also acts as one of the most attractive techniques for processing nano-hybrid and nanocomposite materials [64-65].

The solvothermal processing of materials is a part of solution processing and it can be described as super heated aqueous solution processing. This process takes place in a liquid medium above the boiling point and 1 bar. Crystallization by solvothermal synthesis is, in the simplest case, a straight forward (isothermal) equilibrium reaction. Substances that are insoluble under ambient conditions are dissolved, and the crystalline phase, which is stable under the solvothermal conditions, is formed. Most of the solvothermal processes are carried out in water, and

thus are termed hydrothermal. Besides water, alcohol, ammomia and others are the most important solvothermal reaction medium (The solvent in the solution phase is inclined to transport the species from the small crystallites to larger one).

For processing nanomaterials, the solvothermal technique offers special advantages because of the highly controlled diffusivity in a strong solvent media in a closed system.

The advantages of solvothermal are summarized as follow:

(1) Reactants, which are normally volatile at the required reaction temparatures, tend to condense during solvothermal process maintaining the reaction stoichiometry and high product purity and homogeneity, narrow particle size distributions of the products are obtained.

(2) It is a low temperature process, with many effects achievable even below 300 ^{o}C. The relatively low temperature can break down the stable precursors under pressure, which avoids the extensive agglomerations that the solid – state reaction usually cause at high temperature.

(3) The synthesis is accomplished in a closed system from which different chemicals can be recovered and recycled. That makes it an environmentally benign process.

The disadvantages of this process are:

(1) The moderately high initial cost of the apparatus

(2) Safety issues related to high pressure processing

(3) Corrosion problem may be arising in the presence of acidic and basic medium.

Figure 1.11 General purpose autoclave popularly used for hydrothermal synthesis

There are several hundreds of reports on metal sulfides such as CdS, PbS, ZnS, CuS, NiS, NiS_2, NiS_7,Bi_2S_3, $AgIn_5S_8$, MoS, FeS2, InS, Ag_2S, and so on, prepared through hydrothermal or solvothermal routes with or without capping agents/surfactants/additives to alter their morphologies and sizes as desired [64].

1.3.6 Templated synthesis

We have known that various properties of materials depend on their morphology. Many methods have developed in order to prepare nanomaterials ranging from solid state reaction, chemical synthesis and lithographic method. However, it still has a weakness that is unable to control final morphology.

The template methods represent the most commonly used methods for the synthesis of anisotropic structures. In this approach, the template simply serves as a scaffold within which a different material is generated in situ and shaped into a nanostructure with morphology complementary to that of the template. Many different templates have been successfully designed for the synthesis of anisotropic nanoparticles. The hard templates include inorganic mesoporous materials such as

anodic aluminium oxide (AAO) and zeolites, mesoporous polymer membranes, block copolymers, carbon nanotubes, etc. [66]. Soft templates generally refer to surfactant assemblies such as monolayers, liquid crystals, vesicles, micells, polymers, etc. [67] The template-directed approach provides a simple and cost-effective procedure that allows the complex topology present on the surface of the template to be duplicated in a single step.

1.4 Characterization techniques for nanostructured materials

In the previous part, methods for the synthesis of metal sulfides nanostructures were presented. Along with the synthesis and fabrication processes, the nanomaterials need to be characterized to assess their physical and chemical properties. When dimensions of material are reduced to nanoscale they demonstrate unique properties which are different from those of their bulk counterparts. For example, their electronic and optical properties alter, their chemical activities can be increased or decreased and mechanical/structural stabilities are changed. Such features make nanomaterials attractive for unique applications, and also at the same time, cause complications in their characterization processes. Therefore, the challenge lies in finding the right characterization techniques that have the optimum capabilities for studying the characteristics of nanomaterials. A large number of techniques can be employed for nanomaterials characterization. Some of the most common characterization techniques in nanotechnology will be presented in this part.

1.4.1 X-ray diffraction (XRD)

XRD involves monitoring the diffraction of X-rays after they interact with the sample. It is a crystallographic technique used for identifying and quantifying various crystalline phases present in solid materials and powders [68-69]. The diffraction of x-rays is a result of scattering from atoms configured in regular arrays. The spacing between atoms and planes of atoms is on the order of the wavelength of the x-rays. Bragg's law forms the foundation for x-ray diffraction:

$$n\lambda = 2d \sin \theta$$

By varying the angle θ, the Bragg Law condition is satisfied for different *d*-spacings in polycrystalline materials. Plotting the angular positions versus intensities produces a diffraction pattern, which is characteristic of the sample. In a typical XRD pattern, the diffracted intensities are plotted versus the detector angle 2θ. Each peak is then assigned a label indicating the spacing of a crystal plane. From such a pattern the crystal phases can be identified by comparison to those of internationally recognized databases (such as *Joint Committee for Powder Diffraction Standard - JCPDS*) that contain reference patterns. The Cu-K_α (0.15416 nm) source is used for most XRD analyses

Bragg's law states the condition for sharp diffraction peaks arising from crystals which are perfectly ordered. Actual diffraction peaks have a finite width resulting from imperfections, either the irradiation source or the sample. A useful phenomenon is that as crystallite dimensions enter the nanoscale, the peaks broaden with decreasing crystal size. It is known that the widths of the diffraction peaks allow the determination of crystallite size. Practically, the size of crystallites can be determined using variants of the Scherrer equation:

$$t = \frac{K\lambda}{B\cos\theta}$$

where t is the thickness of the crystal, K is a constant which depends on the crystallite shape, and B is the full width at half maximum of the broadened peak.

Traditional x-ray diffraction is appropriately used to obtained structural characteristics of bulk crystals. For nanocrystals, traditional XRD is not always appropriate because the coherence length of the structure is limited. Diffuse XRD patterns are formed from bulk materials that have short coherence range and from glass-materials with no long-range order. Nanomaterials can exhibit a range of periodicity and structural coherence and short size. This also results in diffuse peaks. Extra special techniques need to be applied. High-energy x-ray diffraction (HEXRD) and atomic pair distribution function (PDF) analysis have been shown to be extremely accurate in determining the fine structure of nanomaterials.

In addition, *Small Angle X-ray Scattering Analysis (SAXS)* based on the principle of scattering of x-ray by crystalline and amorphous but uniformly sized small particles (1-100 nm) can be used to characterize the samples. SAXS can be applicable to powders in the dry state, suspended in the medium and thin films. Particle size can also estimate by analyzing the width of Bragg peaks in x-ray diffraction spectra.

1.4.2 Scanning Electron Microscope (SEM)

The SEM is perhaps the most routinely utilized instruments for the characterization of nanomaterials. With an SEM, it is possible to obtain secondary electron images of inorganic materials with nanoscale resolution, allowing topographical and morphological studies to be carried out, by scanning an electron probe across a surface and monitoring the secondary electrons emitted. Compositional

analysis of a material may also be obtained by monitoring X-rays produced by the electron-specimen interaction. Thus, detailed maps of elemental distribution can be produced. A schematic diagram of an SEM is shown in Figure 1.12. [70-71]. The electron beam is emitted from a heated filament, which is commonly made from lanthanum hexaboride (LaB6) or tungsten. The filament is heated by applying a voltage, which causes electrons to be emitted. Alternatively, electrons can be emitted via *field emission* (*FE*). The electrons are accelerated towards the sample by applying an electric potential. This resulting electron beam is focused by a condenser lens, which projects the image of the source onto the condenser aperture. It is then focused by an objective lens and raster-scanned over the sample by scanning coils. This is achieved by varying the voltage produced by the scan generator on the scan coils that are energized, creating a magnetic field, which deflects the beam back and forth in a controlled pattern. When the primary electrons hit the sample, they give part of their energy to electrons in the sample, resulting in the emission of secondary electrons. These secondary electrons have lower energies (around 20 eV). These secondary electrons are collected by an Everhart-Thornley detector, converted to a voltage, amplified and build the image. Their intensity is displayed versus the position of the primary beam on the sample. The samples placed in the SEM must be either conducting or covered with a thin metal layer in order to avoid electric charging. Scanning takes place at low pressures, so that the electrons are not scattered by gas molecules inside the chamber. Furthermore, with an SEM it is possible to obtain images from comparatively large area of the sample. In addition to secondary electrons, there are also high-energy electrons, originating in the electron beam (producing X-rays), that are backscattered from the specimen interaction volume.

These electrons may be used to detect contrast between areas with different chemical compositions.

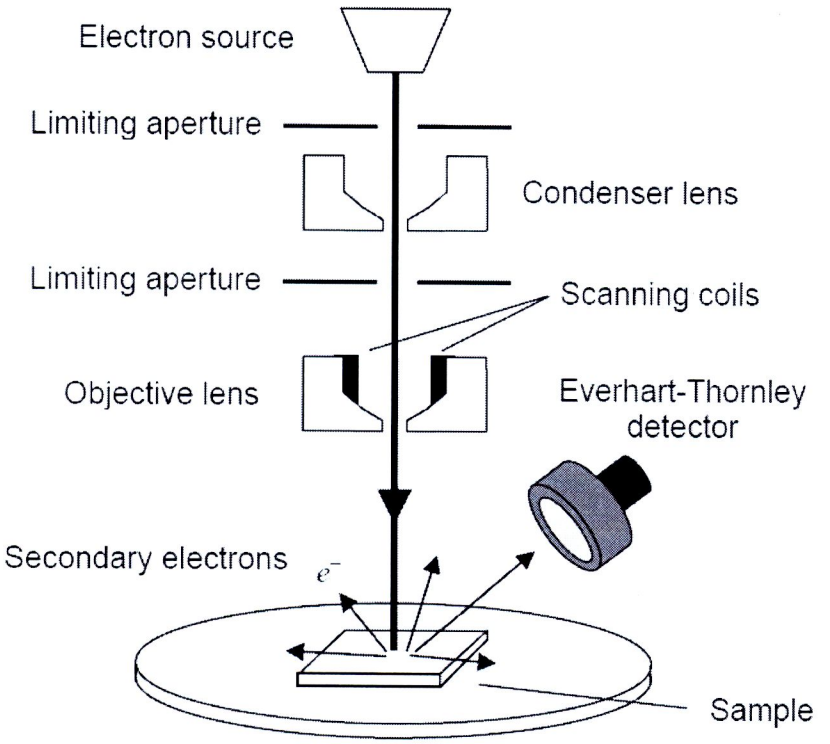

Figure 1.12 Schematic diagram of an SEM set-up [71]

Nowadays SEMs are designed for specific purposes ranging from routine morphological studies, cryogenic studies, to high-speed compositional analyses or for the study of environment-sensitive materials [72-73].

1.4.3 Transmission Electron Microscope (TEM)

In a *TEM*, a beam of focused high energy electrons is transmitted through a thin sample to reveal information about its morphology, crystallography, particle size distribution, and its elemental composition. It is capable of providing atomic-resolution lattice images, as well as giving chemical information at a spatial resolution of 1 nm or better. Because the unique physical and chemical properties of

nanomaterials not only depend on their composition, but also on their structures, TEM provides a means for characterizing and understanding such structures. TEM is unique as it can be used to focus on a single nanoparticle in a sample, and directly identify and quantify its chemical and electronic structure. Perhaps the most important application of TEM is the atomic-resolution real-space imaging of nanoparticles [74]. A TEM operates in a similar manner to a slide projector. As the electron beam passes through the sample, only certain parts of it are transmitted, making an amplitude contract image. The image passes through a magnifying lens and is then projected onto a phosphor screen or a charge coupled device (CCD), which allows for quantitative data processing. Information may also be obtained from backscattered and secondary electrons, as well as emitted photons. A wide variety of materials can be characterized with a TEM, including metals, minerals, ceramics, semiconductors, and polymers. Because electrons must be transmitted through the material this requires that the sample be appropriately thin. A simplified TEM setup is shown in Figure 1.13. The electron gun is a pin shaped cathode that is typically made from materials such as LaB6. Heating this cathode by applying a large current produces a stream of almost monochromatic electrons that travel down a long column after being accelerated by a large voltage. Increasing this voltage increases the kinetic energy of the electrons and hence decreases their wavelength. The smaller the electron beam wavelength the higher the resolution, although the quality of the lens-systems is the limiting factor. The condenser lenses focus the beam to a small and coherent cylinder while the condenser aperture removes electrons scattered at large angles. The beam strikes the specimen on the sample holder, and the majority is transmitted, focused by the objective lens, after which it passes through the intermediate and projector lenses

and enlarged. Eventually by striking a phosphor or CCD surface it forms an image. The TEM has the capability to create both electron microscope images (information in real space) and diffraction patterns (information in reciprocal space) for the same region by adjusting the strength of the magnetic lenses [75]. By inserting a selected area aperture and using parallel incident beam illumination, a selected area electron diffraction pattern from an area as small as several hundreds to a few nm in diameter is obtained. Crystal structures can also be investigated by *high resolution transmission electron microscopy* (*HRTEM*) where the images are formed due to differences in phase of electron waves scattered through a thin specimen. The emergence of *HRTEM* has allowed the direct reconstruction of Bragg differential electron beams to create interference patters, which in favorable cases of simple projected electrons, give a representation of the underlying crystallographic diffraction grating.

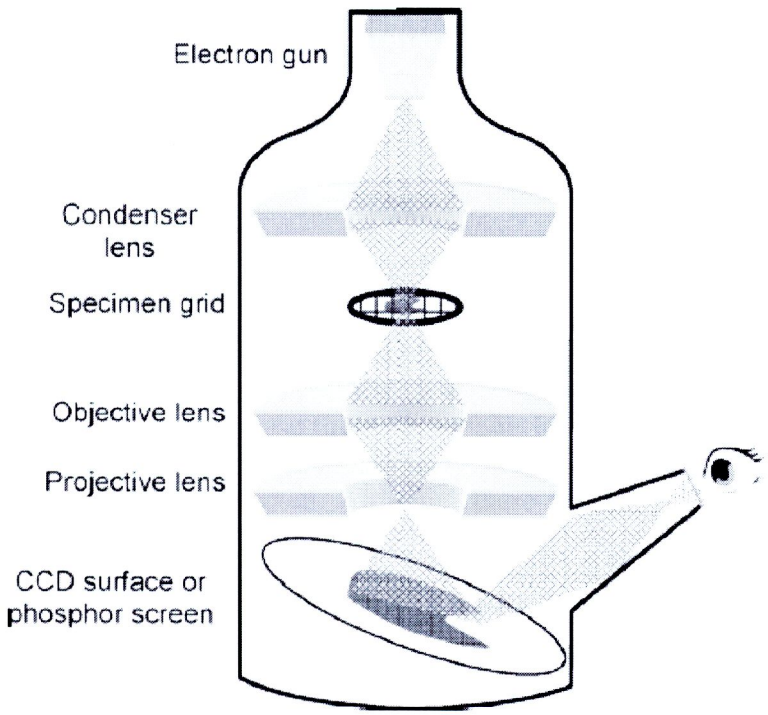

Figure 1.13 Schematic diagram of a TEM set-up [71,75]

Limitations of the TEM procedure include the following:

(1) Extensive sample preparation is time consuming and this limits the number of samples that can be imaged and analyzed.

(2) In addition to the small physical size of samples, the field of view is relatively small as well. For example, the section under analysis may not be representative of the sample as a whole.

(3) Sample structure and morphology have been known to change drastically under exposure to electrons with extremely high energy, and damage samples in particular can occur.

(4) TEM is a high-vacuum instrument that is costly to operate and to maintain, certainly playing a role in the high barrier entry required to conduct nanoscience research.

However, the advantages of the TEM technique are numerous. Any type of sample, whether electrically insulating, semiconducting, or conducting, is able to be imaged by TEM.

1.4.4 Raman and Fourier Transform Infrared (FTIR) Spectroscopy

Raman spectroscopy is a powerful method for the investigation of the structural properties of nanoparticles because the variations in Raman spectra with decreases in particle size can be easily detected. Although there is still some controversy as to what effects variation in particle size has on phonon modes and on the electron-phonon interaction .Raman studies of these materials are useful in two distinct ways. Firstly, it is possible to determine the size of nanoparticles from a measurement of the maximum of the low frequency Raman band. The frequency v (in cm^{-1}) of the lowest-

energy spherical mode of a free particle, corresponding to angular momentum $l = 0$, is given by

$$\nu = \frac{0.7 v_L}{d \times c}$$

where v_L is the speed of the longitudinal sound waves, c is the vacuum light velocity of sound, and d is particle diameter. Secondly, this technique provides valuable information about the surface modes and thus about the effects of the finite size of the nanoparticles, because the surface modes become dominant as particle size decreases due to the increase in the surface-to-volume ratio. Raman spectra of nanocrystals have been studied in a number of cases, including CdS, CdSe, ZnS, InP and etc [76, 77].

Infrared spectroscopy is extremely method used to characterize nanomaterials, especially, their surfaces. This technique measures the absorption of radiation by high frequency (i.e., optical branch) phonon vibrations, and they are sensitive to the presence of particular chemical groups such as hydroxyl (-OH), methyl ($-CH_3$), imido (-NH), amino ($-NH_2$). Each of these groups absorbs infrared radiation at characteristic frequency, and the actual frequency of the absorption varies somewhat with the environment. Not only characterize surface properties of nanomaterials but also reaction mechanism investigation for example T. Thongtem et al. used FTIR to study formation mechanism of copper-thiourea complex. When copper-thiourea complex was produced, the intensity peak in thiourea was diminished in the complex. It was influenced by a change in the nature of C = S and C–N bonds due to the complex formation [78].

1.4.5 UV-NIR spectroscopy

UV-NIR spectroscopy is widely utilized to characterize organic molecules and inorganic nanostructure. A sample is irradiated with electromagnetic waves in the ultraviolet, visible and near IR ranges and the absorbed light is analyzed through the resulting spectrum [79]. The samples can be either organic or inorganic, and may exist in gaseous, liquid or solid form. Herein, the used of this technique for characterizing inorganic nanomaterials will be mentioned. Size dependant properties can be observed in the spectrum, particularly in the nano and atomic scales. These include peak broadening and shifts in the absorption wavelength. Many electronic properties, such as the band gap of a material, can also be determined by this technique. The energies associated with UV-NIR ranges are sufficient to excite electrons from valance band (HOMO) to conduction band (LUMO). Photons in the visible range have wavelengths between 800-400 nm, which corresponds to energies between 1.55 and 3.10 eV. The near UV range includes wavelengths down to 200 nm, and has energies as high as 6.20 eV. The near IR region covers wavelengths between 800-1500 nm (1.55-0.83 eV). As a result, UV-NIR spectroscopy is an ideal technique for determining the electronic properties of both large and narrow band gap nanomaterials. In the spectrum of nanoparticles, the absorption peak's width strongly depends on the particle sizes and shapes. As a result, their spectrum is different from their bulk counterparts. For instance, for semiconductor nanocrystals, the absorption spectrum is broadened owing to quantum confinement effects and as their size reduces [80-81]. Furthermore, semiconductor nanoparticles's absorption peaks shift towards smaller wavelengths (higher energies) as their crystal size decreases [82-84]. An important consequence of using this technique is that the band gap of nanosized

materials can be determined. For semiconductors, a classical Tauc approach was employed to estimate their optical energy band gaps using the following equation:

$$h\nu\alpha = A(h\nu - E_g^{opt})^{m/2},$$

where A is a constant, α is the absorption coefficient ,and m equals 1 or ½ for a direct transition and indirect band gap, respectively. h is the Planck constant, v is the frequency, and E_g^{opt} is the optical band gap. A plot of $(h\nu\alpha)^2$ against $(h\nu)$ for a direct transition. The value of $(h\nu\alpha)^2$ extrapolated to $\alpha = 0$ gives an optical band gap

The consequence of E_g is that we can use it to investigate the position of valance band energy, which is an important data for photocatalytic application, by using the following equation:

$$E_{VB} = X - E^e + 0.5E_g$$

where E_{VB} is the valance band edge potential, X is the electronegativity of the semiconductor which is the geometric mean of the electronegativity of the constituent atoms, E^e is the energy of free electrons on the hydrogen scale (≈4.5 eV), and E_g is the band gap energy of the semiconductor [85].

1.4.6 Photoluminescence Spectroscopy (PL)

PL spectroscopy concerns monitoring the light emitted from atoms or molecules after they have absorbed photons [86]. PL spectroscopy is suitable for the characterization of both organic and inorganic materials of virtually any size and shape, and the samples can be in solid, or liquid. Electromagnetic radiation in the UV and visible ranges is utilized in PL spectroscopy. The sample's PL emission properties are characterized by four parameters: intensity, emission wavelength, bandwidth of the emission peak, and the emission stability [87]. Nanomaterials with PL effects, in particular nanocrystals, can reveal many interesting and improved

optical properties. These include brighter emission, narrower emission band, and broad UV absorption. For example, semiconductor nanocrystals produce narrower emission peaks than luminescent organic molecules, with bandwidth of around 30-40 nm. Having a smaller bandwidth, it is much easier to discriminate individual wavelengths emanating from multiple sources, such as in an array of nanocrystals. The PL emission intensities and wavelengths are dependent on particle size. Hence, PL spectroscopy directly enables particle size effects, in particular those in the nanoscale, to be observed and quantified [88-89].

As mentioned above, the emission is a result of photoexcitation of the material. The energy of the emitted photons is usually lower than the energy of the incident excitation photons and this emission is considered as the Stokes emission. This is schematically illustrated in Figure 1.14.

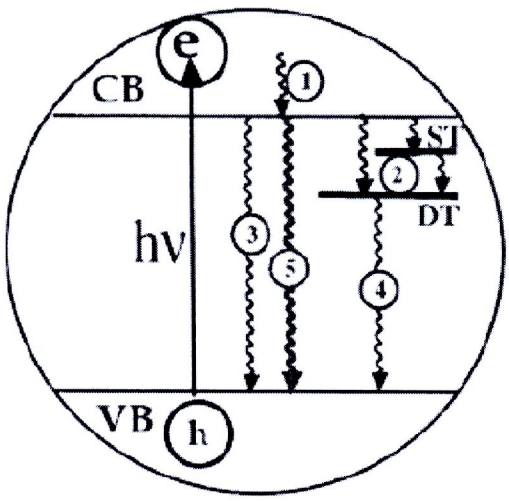

Figure 1.14 Schematic illustration of photoexcitaion in PL (upward arrow) [87]

Figure 1.14 shows the photoexcitation (upward arrow) and relaxation processes. The curve lines with downward arrows indicate different relaxation processes: (1)

electronic relaxation within the conduction band (CB), (2) trapping into shallow trap (ST) and deep trap (DT) state as well as further trapping from ST to DT, (3) band egde electron-hole recombination, (4) trapped electron-hole recombination, and (5) exciton-exciton annihilation.

Photoluminescence can be generally divided into band edge emission, including excitonic emission, and trap state emission. Trap state emission is usually red shifted compared to bandedge emission. For instance, in Figure 1.14, the emission spectrum clearly shows both trap state and bandedge emission with the latter at a shorter wavelength. The ratio between the two types of emission is determined by the density and distribution of trap states. A high trap state emission indicates a high density of trap states and efficient trapping. It is possible to prepare high quality samples that have mostly bandedge emission when the surface is well capped. For example, TOPO capped CdSe show mostly bandedge emission and weak trap state emission, which is an indication of high quality of the sample [90]. Luminescence can be enhanced by surface modification or using core/shell structures. Nanoparticles that have been found to show strong PL include CdSe, CdS, ZnS. Other nanoparticles have generally been found to be weakly luminescence or non-luminescent at room temperature, for example, PbS, PbI, CuS, and Ag_2S. The low luminescence can be due to either indirect nature of the semiconductor or a high density of internal and/or surface trap states that quench the luminescence. The luminescence usually increases at lower temperature due to suppression of electron–phonon interaction and thereby lengthened excited electronic state lifetime. Controlling the surface by removing surface trap states can lead to significant enhancement of luminescence as well as of the ratio of bandedge over trap state emission. The surface modification often

involves capping of the particle surface with organic, inorganic or biological molecules or ions that can result in reduction of trap states that fall within the band gap and quench the luminescence. This scheme of surface states reduction and luminescence enhancement is important for many applications that requires high luminescence yield of nanoparticles, for example, laser, LEDs, fluorescence imaging, and optical sensing [91-93].

1.5 Literature reviews

Byrappa et al. [64] have described the preparing of advanced materials by using solvothermal technology. Solvothermal reactions will proceed in a liquid medium above the boiling point and 1 bar pressure. This technique has a lot of advantages due to the adaptability of the technique and also environmental benign. The great advantages of solvothermal techniques for preparing nanomaterials are the production of materials that are monodispersed with total control over the shape and size including their chemical homogeneity with highest dispersibility. A variety of advanced materials such as metal oxides, semiconductors including II-VI and III-V compounds, silicates, sulfides and tungstates have been processed using the solvothermal technique. In addition, this technique can be used for multi-energy system like microwave-solvothermal, electrochemical-solvothermal or mechanochemical-solvothermal. The use of capping agent, surfactants and other organic molecules contribute greatly to the surface modification to obtain the desired phisico-chemical characteristics. The solvothermal route is more popular than all the others because of the lower temperature, shorter experimental duration and control over the size and morphology. The experiments are usually carried out in the temperature range 150-200 ^{o}C.

Thongtem et al. [94] have prepared CdS (hexagonal structure) with different morphologies by the reaction of cadmium chloride and thiourea in different solvents (benzene, toluene, p-xylene, cyclohexane and tetrahydrofuran). It was found that solvents polarities were play a significant role in shape and size of the final products. Photoluminescence spectra of the obtained products were blue shifted in comparison with the bulk CdS. Furthermore, they also found that photoluminescence intensity of the rod shaped crystal synthesized in tetrahydrofuran was at the highest.

Sun et al. [95] have successfully synthesized CdS nanoparticles and nanorods via a solvothermal method combined with ultrasonic treatment. Cadmium chloride and thioacetamide were selected as starting materials, water and n-haptane as a solvent. It was found that treatment temperature and heating time were the major variables to control the crystal phase, size and morphology of CdS nanocrystalline.The crystal structure of CdS was completely transformed from cubic to hexagonal structure at 150 ^{o}C for 1.5 h. As the temperature and time were increased, the particle size of CdS was increased and its morphologies varied from spherical to rod shape. In addition, this effect can promote the red shift of fluorescence emission of the sample.

Zhang et al. [96] have prepared CdS nanorods in microemulsions formed by non-ionic surfactant TX-100 and cosurfactant hexanol with cadmium chloride and thiourea as the cadmium and sulfur sources, respectively. It was found that the obtained CdS nanorods were very uniform with their sized of 15-30 nm in diameter and 40-300 nm in legth depending on the reaction condition, for example concentration of reactants, water content, types of cadmium salt and acidic media, temperature and composition of the microemulsions.

Chen et al. [97] have prepared CdS and CdSe nanorods via a simple solution-phase route with CTAB as a surfactant. It was found that both CdS and CdSe had a rod-like shape. Selected-area electron diffraction (SAED) showed wurtzite CdS and zincblend CdSe. The EDS analyser was used to confirm that the final products really had 1:1 ratio of Cd : S or Cd : Se. The nanorods with different aspect ratios were obtained by using different amount of cyclohexane in micellar solution. These results showed that cyclohexane played an important role in the formation of nanorods.

Ji et al. [98] have synthesized CuS nanocrystals with various morphologies such as nanorod, nanoflake and nanoflower using hydrothermal method. In this process, they used PEG20000 (nonionic surfactant) as a shape-controller agent. They found that PEG20000 and the reaction temperature played important role in controlling the morphologies of CuS products. In addition, the different morphologies of the products would be expected to have a promising for advance materials.

Nagurathinam et al. [99] have successfully synthesized covellite CuS nanocrystal by using Cu (II) coordination polymer, and $[Cu(HSglu)(H_2O)].H_2O$ as a precursor and a sacrificial template. They investigated the effect of several reaction parameters on the morphologies and size of the products. At appropriate condition, petal-bed-like morphology, flower like and rice-ball-like morphology have been successfully achieved. In addition, they believed that careful investigation of the packing pattern of the coordination in the crystal lattice leads to synthesize nanomaterials with inexpensive, eco-friendly, simple synthetic procedure and with definite shape and size.

Zhang et al. [100] presented a novel approach to synthesize single crystalline, monodisperse copper sulfide nanocrystal. Reaction proceeded via high-temperature chemical reaction of $CuCl_2$ and S in oleylamine (OLA). They also investigated the effect of molar ratio of [$CuCl_2$]: [S] on size and shape of the products. When molar ratios of [$CuCl_2$] : [S] were 1:1, 2:3 and 2:1, the hexagonal CuS nanodisks, hexagonal CuS nanoribbons consisting of face-to-face stacked nanodisks and monoclinic $Cu_{1.75}S$ nanoribbons consisting of face-to-face stacked nanodisks were obtained, respectively.

Wang et al. [101] obtained hexagonal nanoplates of CuS through chemical vapor reaction in which sulfur vapor reacted with copper film in vacuum chamber at about 450 ^{o}C for 7h. They also studied the effect of film thickness, reaction time and temperature. At appropriate condition, the CuS hexagonal nanoplates were single crystal with an edge length of 0.2-1.8 μm and 20-150 nm in thickness.

Zhang et al. [102] reported the synthesis of Bi_2S_3 flower-like structure via a facile solution-phase biomolecule - assisted approach. The morphologies, structure and phase composition of the obtained products were characterized using various techniques such as SEM, XRD, XPS, TEM, SAED and HRTEM. At appropriate conditions, the obtained Bi_2S_3 nanorod with flower like homogeneous assemblies were highly crystalline and grew along the [001] direction. They found that the capacity of electrochemical hydrogen storage was susceptible to this morphology as well.

Ma et al. [103] have prepared Bi_2S_3 nanorod using a surfactant-assisted solvothermal method. The products characterized by XRD, HRTEM showed pure orthorhombic structure with preferential growth in the [001] direction. In addition,

they found that the optical properties of the products were strongly influenced by surfactant (SDS and Span 80).

Quan et al. [104] have successfully prepared single crystalline Bi_2S_3 with various morphologies such as wires, rods and flowers via a polyol solution process. The morphologies of the products were dependent of the experimental parameters including the reaction temperature, prolonged time, reactant ratio, sulfur source and additive. They found that excess S source was favorable for the formation of high quality Bi_2S_3 nanostructure. The dimensions of Bi_2S_3 were highly dependent of the nature of S sources. They also proposed a possible mechanism for the formation of Bi_2S_3 nanotructures.

Zhu et al. [105] have synthesized bismuth sulfide with various morphologies via a hydrothermal process. They used $Bi(NO_3)_2.5H_2O$ and $CS(NH_2)_2$ as a precursor and KOH as a mineralizer. The PL emission intensity of the product prepared using KOH as mineralizer (uniform rod-shape) was much higher than KOH-free solution (irregular and agglomeration particles). Finally, they summarized that the optical property of Bi_2S_3 depends strongly on their morphologies.

Wang et al. [106] have successfully synthesized stibnite (Sb_2S_3) nanorods with diameters of 20-40 nm and lengths of 220-350 nm using sonochemical method. The reaction proceeded under ambient air from an ethanolic solution containing antimony trichloride and thioacetamide. The used of various techniques such as XRD, XPS, SEM, EDX, TEM, SAED and HRTEM revealed that the Sb_2S_3 nanorods crystallize in an orthorhombic structure and preferentially grew along the [001] direction. From the results, they divided the formation of stibnite nanorods into four steps: (1) ultrasound-induced decomposition of the precursor, which leads to the formation of amorphous

Sb_2S_3 nanospheres; (2) ultrasound-induced crystallization of these amorphous nanospheres and generation of nanocrystalline irregular short rods; (3) a crystal growth process, giving rise to the formation of regular needle-shaped nanowhiskers; and (4) surface corrosion and fragmentation of the nanowhiskers by ultrasound irradiation, resulting in the formation of regular nanorods. The band gap energy of Sb_2S_3 nanorods investigated using reflection spectroscopy was measured to be 1.94 eV.

Bao et al. [107] have synthesized single crystal antimony sulfide nanowires and studied their electrical transport properties. They synthesized the nanowires using a facile organic molecule-assisted hydrothermal method. Such nanowires preferentially grew along the [001] direction. The individual nanowire exhibited nonlinear IV curve, indicating its potential application in electronic nanodevices.

Chen et al. [108] have prepared rod - like antimony sulfide (Sb_2S_3) dendrite using hydrothermal method at 160 ^{o}C for 12h. They used antimony chloride, thioacetamide and citric acid as raw materials. By using XRD, the orthorhombic Sb_2S_3 with lattice parameters a = 1.120 nm, b = 1.128 nm, c = 0.3803 nm was detected. TEM images showed dendrite-like Sb_2S_3 which was composed of nanorods with the length of 5-20 μm and 300-500 nm in diameter. In addition, they postulated that the rod-like morphology was formed due to its inherent chain type structure and crystal splitting growth.

1.6 Research Objectives

1.6.1 To develop the synthesis of metal sulfides with specified shape and size using a growth controlling agents – assisted solvothermal methods

1.6.2 To investigate and characterize the properties of the metal sulfides

1.6.3 To study the effect of growth controlling agents on the product morphologies

1.6.4 To study mechanism for growth controlling agents - assisted solvothermal synthesis

1.7 Usefulness of the Research (Theoretical and/or Applied)

1.7.1 Metal sulfides nanostructures which have unique chemical and physical properties will be synthesized.

1.7.2 The synthetic technique of the materials is able to apply for other large scale productions.